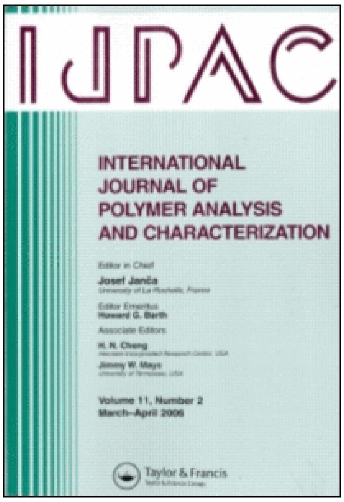

International Journal of Polymer Analysis and Characterization
Publication details, including instructions for authors and subscription information:
http://www.informaworld.com/smpp/title~content=t713646643

Thermal Degradation of Bisphenol A Type Novolac Epoxy Resin Cured with 4,4'-Diaminodiphenyl Sulfone

Yanfang Liu[a]; Zhongjie Du[a]; Chen Zhang[a]; Hangquan Li[a]
[a] Key Laboratory of Beijing City on Preparation and Processing of Novel Polymer Materials, School of Materials Science and Engineering, Beijing University of Chemical Technology, Beijing, China

To cite this Article Liu, Yanfang , Du, Zhongjie , Zhang, Chen and Li, Hangquan(2006) 'Thermal Degradation of Bisphenol A Type Novolac Epoxy Resin Cured with 4,4'-Diaminodiphenyl Sulfone', International Journal of Polymer Analysis and Characterization, 11: 4, 299 — 315

To link to this Article: DOI: 10.1080/10236660600750224

URL: http://dx.doi.org/10.1080/10236660600750224

International Journal of Polymer Anal. Charact., 11: 299–315, 2006
Copyright © Taylor & Francis Group, LLC
ISSN: 1023-666X print
DOI: 10.1080/10236660600750224

Thermal Degradation of Bisphenol A Type Novolac Epoxy Resin Cured with 4,4′-Diaminodiphenyl Sulfone

Yanfang Liu, Zhongjie Du, Chen Zhang, and Hangquan Li
Key Laboratory of Beijing City on Preparation and Processing of Novel
Polymer Materials, School of Materials Science and Engineering,
Beijing University of Chemical Technology, Beijing, China

Abstract: The curing reaction of bisphenol A type novolac epoxy resin (bis-ANER) with 4,4′-diaminodiphenyl sulfone (DDS) was investigated with Fourier-transform infrared (FTIR) spectroscopy. It was found that the obvious structure changes involve the disappearance of epoxide groups and increase of hydroxyls. Thermal degradation of the bis-ANER/DDS network was studied with thermogravimetry in both dynamic air and nitrogen atmospheres. The degradation takes place in two steps in air but in only one step in nitrogen. FTIR measurement was carried out to identify the changes in the structure during the degradation at different steps. In addition, the thermal degradation reaction mechanism of bis-ANER/DDS with the Coats-Redfern method showed that the kinetic model function of the thermal degradation obeys the Avrami-Erofeev model equation, that is, $g(\alpha) = [-\ln(1-\alpha)]^{2/3}$.

Keywords: Curing reaction; Degradation kinetics; Elemental analysis; Epoxy resin; FTIR; GPC; NMR; Thermogravimetry

Received 9 December 2005; accepted 11 April 2006.

Address correspondence to Hangquan Li, Key Laboratory of Beijing City on Preparation and Processing of Novel Polymer Materials, School of Materials Science and Engineering, Beijing University of Chemical Technology, Beijing 100029, China. E-mail: hli45@yahoo.com.cn

INTRODUCTION

With excellent mechanical, thermal, and electrical properties, epoxy resins are widely used in high-performance structural applications, especially as the matrix of fiber-reinforced composites. Bisphenol A type novolac epoxy resin (bis-ANER) is a high functionality solid polymeric epoxy resin, with excellent properties in terms of thermal stability, and it can be used as the matrix for high-performance fiber-reinforced composites in the aerospace industry and as encapsulant for electronic components.[1–3] A systematic study on the thermal properties and stability of such networks may be significant to their application.

In this study, the curing reaction of bis-ANER with 4,4′-diaminodiphenyl sulfone (DDS) system was investigated with Fourier-transform infrared (FTIR) spectroscopy. Thermal degradation of bis-ANER/DDS network was studied with thermogravimetric analysis (TGA) in both dynamic air and nitrogen atmospheres. The structure changes during the degradation were characterized with FTIR, and the reaction mechanism and the apparent activation energy of the thermal degradation reaction for bis-ANER/DDS network were evaluated with the Flynn-Wall-Ozawa and Coats-Redfern methods.[4–6]

EXPERIMENTAL SECTION

Materials

Bisphenol A, formaldehyde (37 wt% aqueous), and n-butanol were obtained from Beijing Chemical Co. (China). Epichlorohydrin, oxalic acid, sodium hydroxide, and benzene were obtained from Tianjin Chemical Co. (China). Tetrabutylammonium bromide and DDS were obtained from Shanghai Chemical Co. (China). All solvents were used as received without further purification.

Synthesis of bis-ANER

To a 100 mL, three-necked, round-bottomed flask equipped with a mechanical stirrer and a reflux condenser, bisphenol A (22.8 g, 0.1 mol) and n-butanol (25 mL) as a solvent were added. The mixture was first heated to 80°C with stirring, until the bisphenol A was completely dissolved; the solution was allowed to cool to room temperature and then formaldehyde (37 wt% aqueous, 8.1 g, 0.1 mol) and oxalic acid (0.26 g, 0.002 mol) as catalyst were added. Subsequently, the flask was kept between 95° and 100°C to carry out the condensation for 6 h. The generated water and the n-butanol were distilled off at atmospheric pressure first and then under reduced

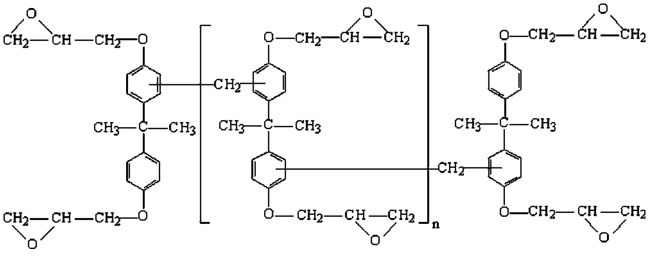

Scheme 1. Molecular structure of bis-ANER.

pressure with the temperature being kept below 150°C. The product was washed several times with boiling water to remove the impurities and unreacted bisphenol A. Finally, water was removed under reduced pressure and 18.9 g of light-yellow transparent solid bisphenol A novolac resin (bis-ANR) product was obtained.[7–9]

To a 100 mL, three-necked, round-bottomed flask equipped with a mechanical stirrer and a reflux condenser, 6.5 g of the previously synthesized bis-ANR, 30 mL of epichlorohydrin, and 0.15 g of tetrabutylammonium bromide as a catalyst were added. The mixture was first allowed to react with stirring at about 100°C for 3 h. Thereafter, the resulting mixture was cooled down to 55°–60°C, which was followed by adding 25 mL of 10 wt% NaOH (aqueous) dropwise through a dropping funnel with stirring over 1.5 h. After the addition of sodium hydroxide, the reaction was continued for an additional 1 h at 65°–70°C. Subsequently, the system was washed with water several times to remove the formed salts. The excess of epichlorohydrin was evaporated from the organic phase under a reduced pressure, and the remaining system was dissolved in benzene and extracted with water several times. Finally, the organic phase was distilled to remove benzene and water, and 9.3 g of light-yellow transparent solid bis-ANER product was obtained.[8–10] The molecular structure is shown in Scheme 1.

The epoxy equivalent weight (EEW) of the synthesized bis-ANER is 213 g/eq, which was determined with the hydrochloric acid-acetone titration method.[11] According to the determined EEW value, the bis-ANER and DDS were mixed with a stoichiometric ratio of one epoxy group versus one active hydrogen.

^{1}H-NMR

With deuterated acetone solvent, ^{1}H-NMR (nuclear magnetic resonance) spectra were recorded on a Bruker AV-600 spectrometer, and tetramethylsilane was used as the internal standard. The assignments of the chemical shifts are shown in Table I.

Table I. Assignment of the chemical shifts of ^{1}H-NMR

bis-ANR		bis-ANER	
Chemical shift (ppm)	Assignment of the hydrogens	Chemical shift (ppm)	Assignment of the hydrogens
1.491–1.585	methyl	1.627	methyl
3.817–3.846	methylene bridge	2.695–2.827	methylene in the oxirane ring
6.692–6.728	aromatic	3.282	methine in the oxirane ring
7.016–7.058	aromatic	6.811–6.865	aromatic
8.081–8.684	hydroxyl	7.093–7.161	aromatic

Elemental Analysis

Elemental analysis was performed on a Vario EL III elemental analyzer, and the results are listed in Table II.

Gel Permeation Chromatography (GPC)

The molecular weight and molecular weight distribution of the resins were determined with a Waters gel permeation chromatograph equipped with a 515 HPLC pump, 717 auto sample injector, Styragel (HT3_HT5_HT6E) columns, 2410 refractive index detector, and 996 photodiode array detector (at 254 nm). The separation columns were calibrated with monodisperse polystyrene standards. Table III shows

Table II. Elemental analysis results of bis-ANR and bis-ANER

Resins	C (%)	H (%)	O (%)
bis-ANR	79.2	7.3	13.5
bis-ANER	74.4	7.2	18.4

Table III. Molecular weights and polydispersities of bis-ANR and bis-ANER determined with GPC

Resins	M_n	M_w	M_w/M_n
bis-ANR	1343	1908	1.42
bis-ANER	1422	3174	2.23

the GPC result, namely the number-average molecular weight (M_n), weight-average molecular weight (M_w), and polydispersity index (M_w/M_n) values.

FTIR Spectroscopy

Infrared spectra were obtained on a Bruker Vector 22 FTIR spectrometer. The resin was first mixed with potassium bromide, and the mixture was pressed into a plate, which was used for scanning.

To study the curing reaction, the bis-ANER/DDS sample was first dissolved in trichloromethane, then coated as a thin film on a potassium bromide plate. When the solvent in the film was completely evaporated in vacuum, the potassium bromide plate was scanned with FTIR. Thereafter, the plate was placed in a heated oven with a fixed temperature of 200°C and dynamic nitrogen atmosphere. During the curing reaction at this temperature, the plate was repeatedly withdrawn and cooled in nitrogen atmosphere at regular time intervals for the FTIR scan.

To study the thermal degradation, after being cured at 200°C for 8 h, the potassium bromide plate with bis-ANER/DDS film was placed in an oven with dynamic nitrogen atmosphere and heated at a heating rate of 10°C/min. When the sample was heated to 350°C, the oven was switched off, and then the sample was withdrawn and cooled in nitrogen atmosphere to measure the FTIR. After the FTIR scan was finished, the oven was reheated at the same heating rate, but the sample was not introduced until the temperature of the oven reached the previous temperature of 350°C. Thereafter, the sample was heated to a second temperature, 430°C, withdrawn, cooled, and scanned again. The same procedure was repeated with the oven heated to 500°C.

Thermal Analysis

A Shimadzu TGA-40 thermogravimeter was used to determine the weight loss behavior of the bis-ANER/DDS network during the degradation process. About 10 mg of the bis-ANER/DDS sample cured at 200°C for 8 h was introduced into the thermobalance, and then the thermobalance was heated to 700°C at different heating rates: 2.5°, 5°, 7.5°, 10°, and 12.5°C/min. The experiments were carried out under dynamic air and nitrogen atmospheres at a flow rate of 40 mL/min, respectively.

A Shimadzu DSC-41 differential scanning calorimeter was used to determine the ΔH of the curing reaction of bis-ANER/DDS operating in a nitrogen atmosphere at a flow rate of 40 mL/min. The amount of sample used was about 10 mg, and the sample was scanned at a heating rate of 10°C/min.

A Shimadzu DTA-40 differential thermal analyzer (DTA) was used to measure the heat release behavior of the bis-ANER/DDS network during the degradation process. About 10 mg of the bis-ANER/DDS sample cured at 200°C for 8 h was introduced into the instrument and then heated to 700°C at a heating rate of 10°C/min under dynamic air.

RESULTS AND DISCUSSION

Synthesis and Characterization

Bis-ANR was obtained by the reaction of bisphenol A with formaldehyde with oxalic acid as a catalyst. The preparation of bis-ANER involved the reaction of bis-ANR with a halohydrin in the presence of an alkali metal hydroxide.

The IR spectra of bis-ANR and bis-ANER are shown in Figure 1. For the spectrum of bis-ANR, the absorption at 3342 cm^{-1} was assigned to stretching vibrations of the phenolic hydroxyl group. For the spectrum of bis-ANER, the absorption at 912 cm^{-1} was assigned to the oxirane rings.

The molecular structure of bis-ANER shown in Scheme 1 was confirmed based on the ^{1}H-NMR spectroscopy (Figure 2), elemental analysis, and IR spectroscopy characterizing results.

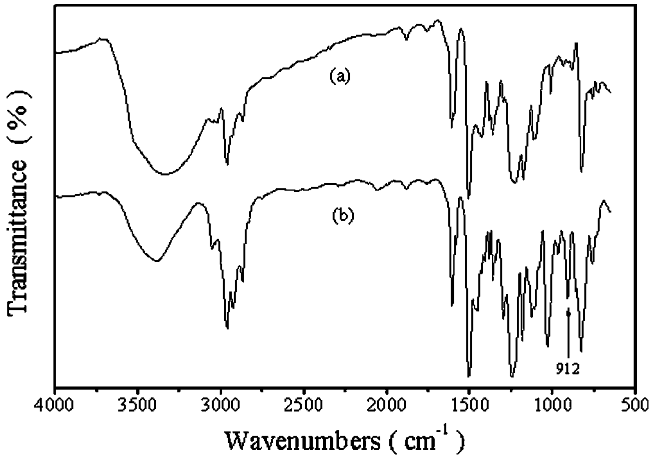

Figure 1. The FTIR spectra of (a) bis-ANR and (b) bis-ANER.

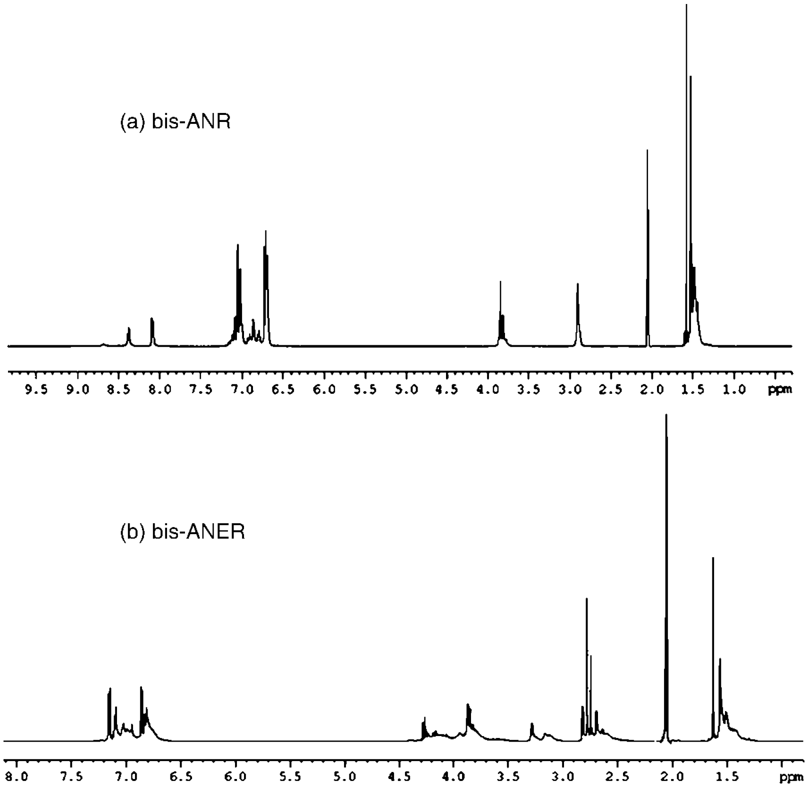

Figure 2. ^{1}H-NMR spectra of (a) bis-ANR and (b) bis-ANER in acetone-d_6.

Curing Reaction

Figure 3 shows the FTIR spectra of the bis-ANER/DDS system during the curing reaction process, which indicated the chemical evolution of the curing reaction. Obvious changes of absorbance can be seen at 912 cm^{-1} for epoxide groups, 3420–3462 cm^{-1} for hydroxyl groups, and 2870–2966 cm^{-1} for alkyl groups. With the evolution of the reaction, the absorption intensity at 912 cm^{-1} decreased while those at 3420–3462 cm^{-1} and 2870–2966 cm^{-1} increased. This phenomenon was attributed to the ring-opening reactions between epoxide groups and active hydrogens. Correspondingly, the absorptions of N–H at 3337 cm^{-1} and 3366 cm^{-1} disappeared quickly in the initial stages of curing, and a gradual increase in the relative absorption intensities at 1105–1142 cm^{-1} for C–O–C was observed. The increase in the absorptions at 1105–1142 cm^{-1} was assigned to the etherification of epoxy with formation of aliphatic ethers.

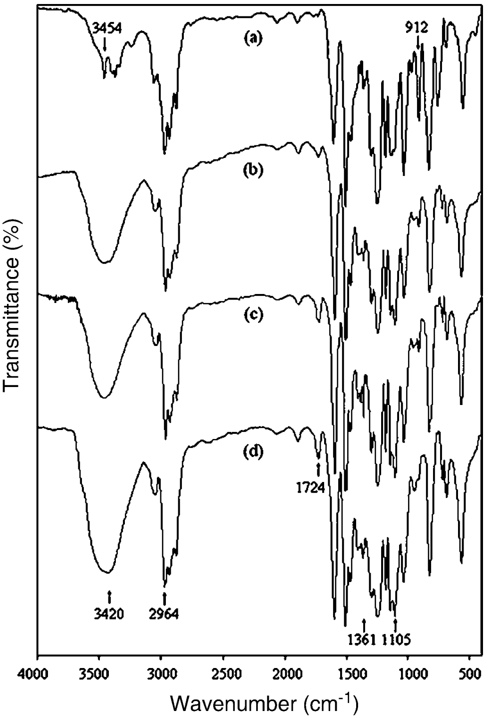

Figure 3. The FTIR spectra of bis-ANER/DDS uncured (a) and cured at 200°C for (b) 1 h; (c) 4 h; (d) 8 h.

After 8 h of curing, the absorption of the epoxide groups at 912 cm^{-1} disappeared completely. In addition, a new absorption feature appeared at 1718–1724 cm^{-1} after 1 h of curing at 200°C, which may be assigned to aldehyde groups generated by epoxide isomerization as shown in Scheme 2.[12,13] The possible epoxide isomerization to form aldehyde had thus been proved,[14] especially for the diffusion-controlled regime in the cure system.

In addition, the curing reaction of bis-ANER/DDS is a heat release process, and the ΔH of the curing reaction determined with DSC was 306.5 J/g.

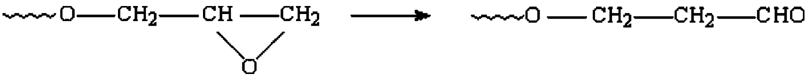

Scheme 2. Isomerization of epoxide during curing reaction process.

Thermal Degradation Behavior

Figure 4 presents the FTIR spectra of bis-ANER/DDS during the thermal degradation process. When the degradation temperature reached 350°C, no apparent changes in the structure of the bis-ANER/DDS network can be seen from the spectra. After the degradation temperature exceeded 430°C, obvious absorbance variations can be seen in the regions of 1035–1142 cm^{-1} for C–O–C and ϕ-S and 3407–3638 cm^{-1} for hydroxyl groups in the spectra. With progressing degradation, the absorption intensities within the two regions gradually weakened. In addition, the absorption intensities at 564 cm^{-1} for SO_2, 824 cm^{-1} for C–H or substituted groups in phenyl ring, 1604 cm^{-1} for phenyl ring, and 2921–2964 cm^{-1} for alkyl groups also weakened when the rising degradation temperature reached 500°C. These changes in characteristic features indicated that the degradation of bis-ANER/DDS could be categorized as two types: those involving the break of weak links, such

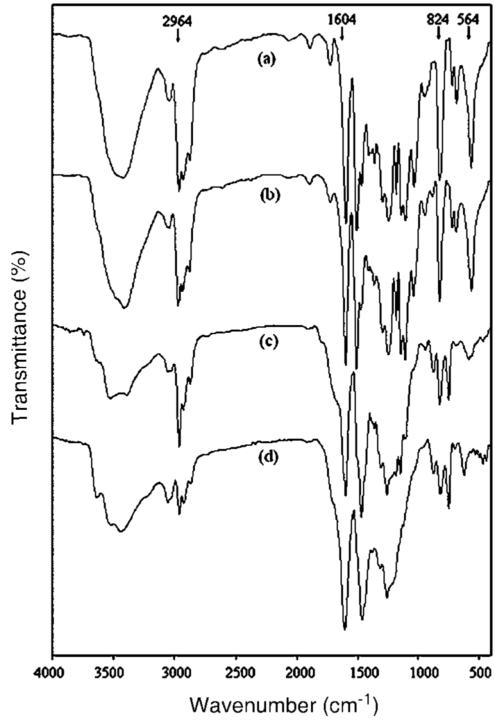

Figure 4. The FTIR spectra of bis-ANER/DDS (a) cured at 200°C for 8 h and afterward heated to (b) 350°C; (c) 430°C; (d) 500°C at a heating rate of 10°C/min in dynamic nitrogen.

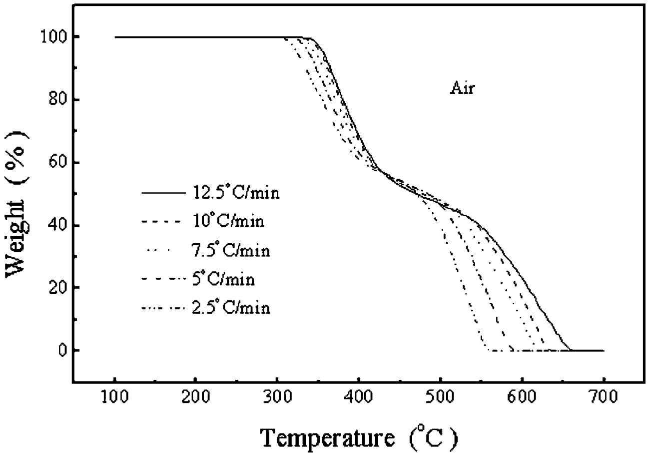

Figure 5. TGA curves of bis-ANER/DDS in dynamic air at different heating rates.

as ϕ-S and C–O–C, and those involving the volatilization or structure conversion of aromatic rings.

Figures 5 and 6 show the weight losses from TGA analysis of bis-ANER/DDS networks in both dynamic air and nitrogen atmospheres. From the curves, two stages of weight loss in air and one stage in nitrogen could be identified. One may notice that about 47% of the gross weight was lost and ended at a temperature of about 430°C in spite of the different atmospheres and different heating rates. Moreover, the degradation

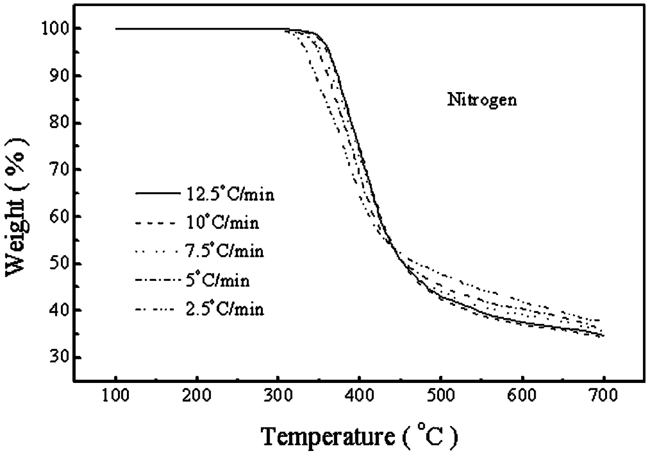

Figure 6. TGA curves of bis-ANER/DDS in dynamic nitrogen at different heating rates.

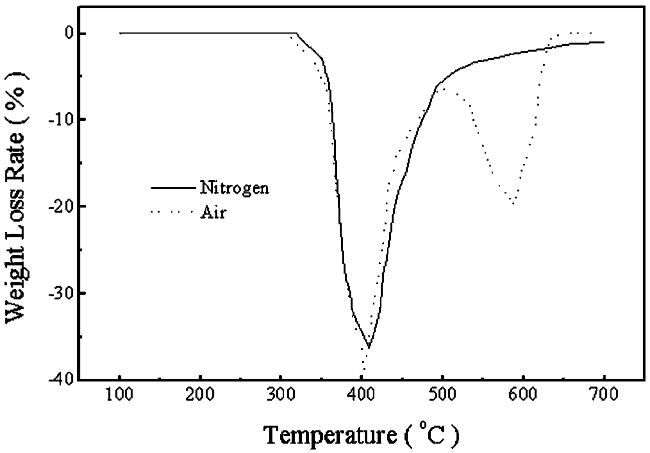

Figure 7. DTG curves of bis-ANER/DDS in dynamic air and nitrogen at a heating rate of 10°C/min.

rates in the two atmospheres were close in the first stage, which can be seen from the DTG curves in Figure 7. Therefore, the effect of oxygen on the first decomposition stage was not obvious in the thermal analysis curves. However, the degradation behaviors in the higher temperatures for the two atmospheres were different. The rate of weight loss in air was faster and the degradation was completed under 660°C, while in nitrogen, it was slower and the weight of the residues leveled off at a finite value. This indicates that oxygen must play an active role at higher temperatures.

When the degradation temperature was under 500°C, weight loss corresponded to the breaking of the weak links, such as ϕ-S and C–O–C, as shown in Figure 4. The effect of oxygen on degradation was not obvious. However, in the subsequent reaction process, the degradation behaviors in the two atmospheres were distinct. According to Figure 4, the subsequent reaction was attributed mainly to the volatilization, structure conversion, or oxidation of aromatic rings. Such reactions should not take place in nitrogen, and for this reason, a limited weight loss in nitrogen was observed while the remains were completely degraded in air. The DTA trace in Figure 8 supports this explanation. Correspondingly, only a minor exothermal peak can be seen for the first weight loss stage in air. This suggests that the detachments of non-carbon were hardly exothermic, and some might be endothermic. However, at higher degradation temperatures, a large peak appeared. Since the corresponding reaction was mainly oxidation, it was natural to observe a release of a large amount of heat.

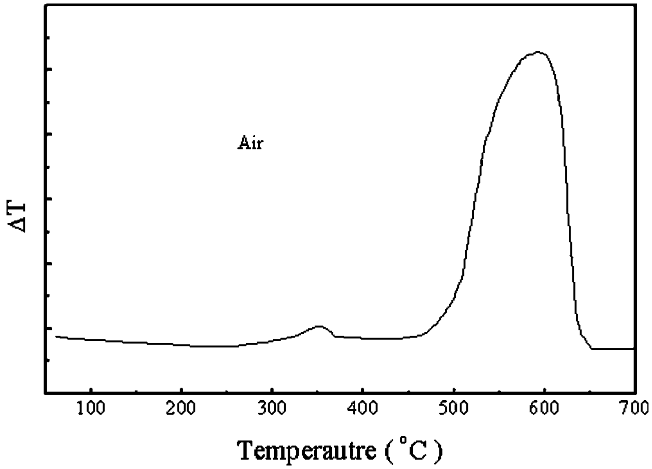

Figure 8. DTA curves of bis-ANER/DDS in dynamic air at a heating rate of 10°C/min.

Thermal Degradation Kinetics

Kinetic information can be obtained from thermogravimetric experiments. To determine the kinetic parameters of degradation from the thermogravimetric data, the first step is to evaluate the conversion of the reaction. In TGA dynamic experiments, the weight change of the sample is regarded as a function of temperature, and the conversion can be expressed as

$$\alpha = \frac{w_i - w_T}{w_i} \tag{1}$$

where w_i is the sample weight in i stage, and w_T is the residual weight of w_i at temperature T. Therefore, using Equation (1), the conversions are calculated for different degradation stages from the TGA curves.

In order to determine the kinetic parameters of the degradation process, many methods have been reported. Among them, the Flynn-Wall-Ozawa method gives the following equation:[4,5]

$$\log\beta = \log\left[\frac{AE}{g(\alpha)R}\right] - 2.315 - \frac{0.457E}{RT} \tag{2}$$

where β is the heating rate, A is the pre-exponential factor, E is the activation energy, T is the absolute temperature, R is the universal gas constant, and $g(\alpha)$ is the function of the conversion. The method was derived from the basic kinetic equations for heterogeneous chemical

Table IV. Thermal degradation activation energies of bis-ANER/DDS determined with the Flynn-Wall-Ozawa method

		Conversion (%)			
		5	10	15	20
Air	E (kJ/mol)	147.3	153.6	162.7	170.9
	Correlation coefficient	0.9921	0.9948	0.9979	0.9983
Nitrogen	E (kJ/mol)	171.8	171.1	206.9	242.6
	Correlation coefficient	0.9907	0.9912	0.9914	0.9955

reactions and therefore has a wide application, as it is not necessary to know the reaction order to determine the kinetic parameters for given values of conversion. The activation energy for different conversion values can be calculated from a log β versus $1/T$ plot. Owing to the fact that this equation was derived using the Doyle approximation, conversion values only in the range 5–20% can be used. In this study, the conversion values 5, 10, 15, and 20% were used. Activation energies corresponding to different conversions are listed in Table IV. The results show that the activation energies in air were lower than those in nitrogen. This indicated that the presence of oxygen could decrease the activation energy of degradation.

In addition, the Coats-Redfern method gives the following equation:[6]

$$\ln\frac{g(\alpha)}{T^2} = \ln\left[\frac{AR}{\beta E}\left(1 - \frac{2RT}{E}\right)\right] - \frac{E}{RT} \tag{3}$$

Using Equation (3), the activation energy for every g (α) function listed in Table V can be obtained for constant heating rates from fitting of $\ln[g(\alpha)/T^2]$ versus $1/T$ plots. As mentioned above, the apparent activation energies are calculated for the conversions in the range of 5–20%. For the degradation reactions in both dynamic air and nitrogen, the conversions were tested for various mechanism functions. Some results are listed in Tables VI and VII, respectively.

As shown in Tables VI and VII, at a given heating rate, the differences between activation energies for different mechanisms vary from 10.6 to 515 kJ/mol, and the correlation values for different mechanisms are different. According to the principle that the probable mechanism has (i) activation energy values close to those determined with the Flynn-Wall-Ozawa method and (ii) high correlation coefficient value and low standard deviation value, the probable mechanism function of the thermal degradation reaction can be deduced from the calculated results: the degradation reaction in air and nitrogen follows $A_{1.5}$

Table V. Algebraic expressions for g(α) for the most frequently used mechanisms of solid-state processes

Symbol	g(α)	Solid state processes
D_1	α^2	One-dimensional diffusion
D_2	$(1-\alpha)\ln(1-\alpha)+\alpha$	Two-dimensional diffusion
D_3	$[1-(1-\alpha)^{1/3}]^2$	Three-dimensional diffusion (Jander equation)
D_4	$(1-2/3\alpha)-(1-\alpha)^{2/3}$	Three-dimensional diffusion (Ginstling-Brounshtein equation)
R_2	$1-(1-\alpha)^{1/2}$	Phase boundary controlled reaction (contracting area)
R_3	$1-(1-\alpha)^{1/3}$	Phase boundary controlled reaction (contracting volume)
$A_{1.5}$	$[-\ln(1-\alpha)]^{2/3}$	Nucleation and growth (Avrami equation)
A_2	$[-\ln(1-\alpha)]^{1/2}$	Nucleation and growth (Avrami equation)
A_3	$[-\ln(1-\alpha)]^{1/3}$	Nucleation and growth (Avrami equation)
A_4	$[-\ln(1-\alpha)]^{1/4}$	Nucleation and growth (Avrami equation)
F_1	$-\ln(1-\alpha)$	Random nucleation with one nucleus on the individual particle
F_2	$1/(1-\alpha)$	Random nucleation with two nuclei on the individual particle
F_3	$1/(1-\alpha)^2$	Random nucleation with two nuclei on the individual particle

Table VI. Kinetic parameters of the first thermal degradation stage of bis-ANER/DDS at the heating rate of 10°C/min in dynamic air

Symbol	E (kJ/mol)	Correlation coefficient	Standard deviation
D_1	458.3	0.9942697	0.086
D_2	466.7	0.9944613	0.086
D_3	475.3	0.9943176	0.089
D_4	469.5	0.9943421	0.088
R_2	230.2	0.9935963	0.046
R_3	232.3	0.9935154	0.046
$A_{1.5}$	152.4	0.9949925	0.021
A_2	113.3	0.9943383	0.019
A_3	71.9	0.9916826	0.016
A_4	51.5	0.9920571	0.011
F_1	236.6	0.9935548	0.047
F_2	15.5	0.9431343	0.010
F_3	41.3	0.9628822	0.020

Table VII. Kinetic parameters of the thermal degradation of bis-ANER/DDS at the heating rate of 10°C/min in dynamic nitrogen

Symbol	E (kJ/mol)	Correlation coefficient	Standard deviation
D_1	501.3	0.9981412	0.087
D_2	508.1	0.9983710	0.082
D_3	515.0	0.9983836	0.083
D_4	510.4	0.9983721	0.082
R_2	250.5	0.9982737	0.042
R_3	252.2	0.9982156	0.043
$A_{1.5}$	166.9	0.9983322	0.027
A_2	122.6	0.9985914	0.018
A_3	78.2	0.9980667	0.014
A_4	56.0	0.9983141	0.009
F_1	255.7	0.9984488	0.04
F_2	10.6	0.9289861	0.012
F_3	31.7	0.9660681	0.024

Table VIII. Activation energies of the first thermal degradation stage of bis-ANER/DDS at different heating rates in dynamic air

Heating rate (°C/min)	E (kJ/mol)	Correlation coefficient	Standard deviation
2.5	138.5	0.9936581	0.026
5	144.3	0.9949263	0.038
7.5	147.8	0.9958279	0.032
10	152.4	0.9949925	0.021
12.5	155.7	0.9958316	0.043

Table IX. Activation energies of the thermal degradation of bis-ANER/DDS at different heating rates in dynamic nitrogen

Heating rate (°C/min)	E (kJ/mol)	Correlation coefficient	Standard deviation
2.5	145.7	0.9995971	0.011
5	161.0	0.9975365	0.021
7.5	161.1	0.9971294	0.037
10	166.9	0.9983322	0.027
12.5	172.0	0.9907401	0.052

mechanism, that is, $g(\alpha) = [-\ln(1-\alpha)]^{2/3}$. Correspondingly, the kinetic parameters are listed in Tables VIII and IX for the $A_{1.5}$ mechanism function at different heating rates in air and nitrogen, respectively.

As shown in Tables VIII and IX, with the same thermal degradation mechanism, differences exist between the activation energy values for different heating rates in air and in nitrogen.

CONCLUSIONS

Curing reaction of bisphenol A type novolac epoxy resin (bis-ANER) with 4,4′-diaminodiphenyl sulfone (DDS) studied by using Fourier-transform infrared (FTIR) spectroscopy shows that the obvious structure changes involve the disappearance of epoxide groups and increase of hydroxyls.

The thermal degradation reaction takes place in two steps in air and one step in nitrogen, and the main changes occur between 310° and 450°C. The degradation begins with the breaking of weak groups in the backbone and the substitutions of aromatic rings, such as ϕ-S and C–O–C, then accompanying the volatilization, structure conversion or oxidation of some aromatic rings appears. Finally, all the aromatic rings are volatilized, converted, or oxidized.

The analysis of the solid-state processes mechanism of bis-ANER/DDS with the Coats-Redfern method showed that the kinetic model function of thermal degradation obeys the Avrami-Erofeev model equation for different heating rates, that is, $g(\alpha) = [-\ln(1-\alpha)]^{2/3}$.

REFERENCES

[1] Goto, K., S. Hayashi, T. Saito, T. Kaneko, K. Mitani, K. Wakabayashi, and Y. Takagi. (2003). Epoxy resin composition and prepreg made with the epoxy resin composition. U.S. Patent US20030135011.

[2] Hooper, J. R., R. K. Strother, J. Fish, P. G. Pawling, and G. L. Sauer. (2000). Extremely low viscosity matrix epoxy suffusion resin system. U.S. Patent US6040397.

[3] Taguchi, M., Y. Suzumura, T. Saitou, and A. Itou. (2004). Flame retardant epoxy resin composition, and prepreg and fiber-reinforced composite materials made by using the composition. U.S. Patent US20040034127.

[4] Flynn, J. H. and L. A. Wall. (1966). A quick direct method for the determination of activation energy from thermogravimetric data. *J. Polym. Sci. Part B Polym. Lett.* **4**, 323.

[5] Ozawa, T. (1965). A new method of analyzing thermogravimetric data. *Bull. Chem. Soc. Jpn.* **38**, 1881.

[6] Coats, A. W. and J. P. Redfern. (1964). Kinetic parameters from thermogravimetric data. *Nature* **201**, 68.

[7] Wang, C. S. and J. Y. Shieh. (1998). Synthesis and properties of epoxy resins containing 2-(6-oxid-6H-dibenz <c,e><1,2> oxaphosphorin-6-yl)1, 4-benzenediol. *Polymer* **39**, 5819.

[8] Davies, J., P. Johncock, and D. A. Jones. (1999). Epoxy resins based on the 1,2,3,4-tetrahydroquinoxaline and the 2,3,4,5-tetrahydro-1H-1,5-benzodiazepine ring systems. *Polymer* **40**, 4897.

[9] Wang, C. S. and M. C. Lee. (2000). Synthesis and properties of epoxy resins containing 2-(6-oxid-6H-dibenz(c,e)(1,2) oxaphosphorin-6-yl) 1,4-benzenediol (II). *Polymer* **41**, 3631.

[10] Wang, W. J., L. H. Perng, G. H. Hsiue, and F. C. Chang. (2000). Characterization and properties of new silicone-containing epoxy resin. *Polymer* **41**, 6113.

[11] Jay, R. R. (1964). Direct titration of epoxy compounds and aziridines. *Anal. Chem.* **36**, 667.

[12] Lin, R. H., C. L. Chen, L. H. Kao, and P. R. Yang. (2001). Cure behavior of epoxy resins with different kinds of onium salts as latent thermal catalysts. *J. Appl. Polym. Sci.* **82**, 3539.

[13] Regnier, N., M. Fayos, P. Moreau, E. Lafontaine, and B. Mortaigne. (1999). Cure behavior and thermal degradation mechanisms of epoxy and epoxy-cyanate resins. *Polym. Adv. Technol.* **10**, 637.

[14] Morgan, R. J. and E. T. Mones. (1987). The cure reactions, network structure, and mechanical response of diaminodiphenyl sulfone-cured tetraglycidyl 4,4′-diaminodiphenyl methane epoxies. *J. Appl. Polym. Sci.* **33**, 999.